

B₂N₂-Dibenzo[*a,e*]pentalenes: Effect of the BN Orientation Pattern on Antiaromaticity and Optoelectronic Properties

Xiao-Ye Wang,[†] Akimitsu Narita,[†] Xinliang Feng,^{*,‡} and Klaus Müllen^{*,†}

[†]Max Planck Institute for Polymer Research, Ackermannweg 10, 55128 Mainz, Germany

[‡]Center for Advancing Electronics Dresden (cfaed) and Department of Chemistry and Food Chemistry, Technische Universität Dresden, 01062 Dresden, Germany

S Supporting Information

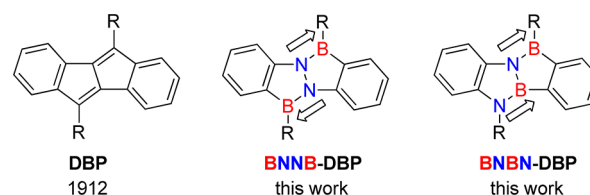
ABSTRACT: Two BN units were embedded in dibenzo[*a,e*]pentalene with different orientation patterns, which significantly modulated its antiaromaticity and optoelectronic properties. Importantly, the vital role of the BN orientation in conjugated molecules with more than one BN unit was demonstrated for the first time. This work indicates a large potential of the BN/CC isosterism for the development of new antiaromatic systems and highlights the importance of precise control of the BN substitution patterns in conjugated materials.

Aromaticity is one of the most important concepts in chemistry. Over decades, aromatic compounds have always been the majority of organic conjugated molecules, whereas antiaromatic ones, which exhibit completely different properties, have been relatively underexplored.¹ Recently, the fundamental interest in BN-substituted benzene, in which a C=C bond is replaced with its isoelectronic B–N bond, has triggered growing research efforts in azaborine chemistry.² The BN/CC isosterism not only expands the structural diversity of organic compounds and enriches the fundamental understanding of aromaticity³ but also provides promising materials for various applications, for example, in hydrogen storage,⁴ biomedicine,⁵ and organic electronics.⁶ A number of BN-substituted aromatic systems have already been reported, including BN-substituted benzene,⁷ naphthalene,⁸ indole,⁹ phenanthrene,¹⁰ anthracene,¹¹ triphenylene,¹² pyrene,¹³ corone,¹⁴ and other polycyclic aromatic compounds.¹⁵ However, the application of this BN substitution strategy in antiaromatic systems has been extremely limited.² On the other hand, in conjugated systems incorporating more than one BN unit, there is a fundamental question about the effect of the BN orientation patterns on their chemical and physical properties. Nevertheless, to the best of our knowledge, there has been no investigation on this topic to date, presumably because of the great challenge of precisely manipulating the BN orientation in the same conjugated skeleton.

Dibenzo[*a,e*]pentalene (DBP) is a ladder-type polycyclic hydrocarbon that possesses antiaromatic character with a $4n\pi$ -electron periphery.¹⁶ Since the first synthesis in 1912, DBPs have attracted considerable research interest regarding the development of convenient synthetic methods and the exploration of their applications in materials science.¹⁷ Herein we chose the DBP skeleton to investigate the effect of BN

substitution on the properties of such antiaromatic systems.¹⁸ We synthesized two B₂N₂-incorporated DBPs with different orientation patterns of BN units (the *anti* orientation, termed **BNNB-DBP**, and the *syn* orientation, termed **BNBN-DBP**; Chart 1). Single-crystal X-ray analysis revealed their planar

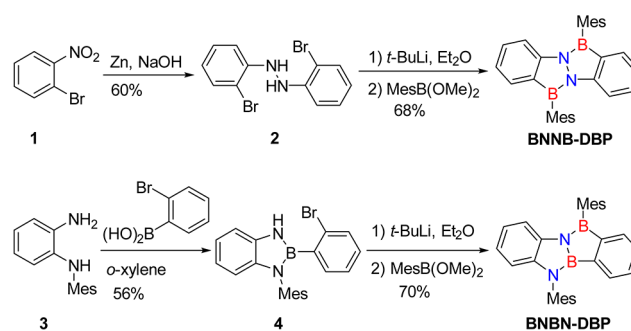
Chart 1. DBP and its BN-Substituted Derivatives



structures, and theoretical, spectroscopic, and electrochemical studies demonstrated that the antiaromaticity and optoelectronic properties are significantly modulated by the different BN substitution patterns.

The synthetic routes to **BNNB-DBP** and **BNBN-DBP** are illustrated in Scheme 1. First, 1-bromo-2-nitrobenzene (**1**) was

Scheme 1. Synthetic Routes to **BNNB-DBP** and **BNBN-DBP**



converted to 2,2'-dibromohydrazobenzene (**2**) under reductive conditions. Then *t*-BuLi was used to perform deprotonations and lithium–halogen exchanges simultaneously at 0 °C to generate a tetralithiated intermediate, which was subsequently reacted with dimethoxymesitylborane to obtain **BNNB-DBP** in 68% yield in one pot. Unlike the electrophilic borylation method used by Cui and co-workers,¹⁸ this approach is not

Received: May 15, 2015

Published: June 5, 2015

affected by the electron density of the reactants and can also avoid high reaction temperatures, making it applicable to a broader scope of substrates. The target compound was stable enough to be purified by column chromatography on silica gel and recrystallization from CH_2Cl_2 /hexane to give colorless crystals. However, when dimethoxyphenylborane was used in the final step, only a complex mixture was obtained, indicating the necessity of bulky protecting groups on the boron center in this nucleophilic substitution step.

The skeleton of the other isomer, **BNBN-DBP**, was constructed in a stepwise manner (Scheme 1). First, *N*-mesitylbenzene-1,2-diamine (**3**) was condensed with (2-bromophenyl)boronic acid in refluxing *o*-xylene to afford precursor **4** in 56% yield. Then lithiation of **4** was performed with *t*-BuLi at $-78\text{ }^\circ\text{C}$ to avoid decomposition of the diazaboroline ring. Subsequent nucleophilic substitution reactions of the dilithiated species with dimethoxymesitylborane afforded **BNBN-DBP** in 70% yield. The solvents played an important role in this step, probably due to the different solubility of LiOMe, which was generated after the ring closure. When THF was used, **BNBN-DBP** could not be obtained, presumably as a result of ring opening of the product caused by nucleophilic attack of the solubilized LiOMe at the unprotected boron, namely, the one not connected to the mesityl group (Scheme S1 in the Supporting Information (SI)). When diethyl ether or dibutyl ether was used as the solvent, LiOMe could be mostly precipitated from the reaction mixture, thus keeping the majority of the product intact. **BNBN-DBP** was less stable than **BNNB-DBP** because of the presence of one unprotected boron, and thus, purification by column chromatography on silica gel or aluminum oxide was unsuccessful, leading to severe hydrolysis. However, **BNBN-DBP** could be purified by careful crystallization from hexane to give a crystalline solid. The solution of **BNBN-DBP** is sensitive to water, so all of the characterizations were performed in freshly dried solvents. In contrast, solid **BNBN-DBP** is stable and can be stored under ambient conditions, showing no change in the ^1H NMR spectra for at least 2 weeks.

The chemical structures of **BNNB-DBP** and **BNBN-DBP** were fully characterized by ^1H , ^{13}C , and ^{11}B NMR spectroscopy as well as high-resolution mass spectrometry. Notably, only one boron signal was observed at 37.3 ppm for **BNNB-DBP**, whereas two signals at 50.4 and 38.3 ppm were recorded for **BNBN-DBP** because of the presence of two kinds of boron atoms. The thermal stabilities of these two compounds were examined by thermogravimetric analysis (TGA), which revealed high decomposition temperatures of $288\text{ }^\circ\text{C}$ for **BNNB-DBP** and $257\text{ }^\circ\text{C}$ for **BNBN-DBP** (Figure S1 in the SI).

BNNB-DBP and **BNBN-DBP** as well as their corresponding precursors were successfully characterized by single-crystal X-ray diffraction. The 6–5–5–6 fused ring structures of **BNNB-DBP** and **BNBN-DBP** can be clearly recognized in Figure 1 as fully planar skeletons. The mesityl substituents are almost perpendicular to the conjugated plane with twisting angles of $70\text{--}80^\circ$. The three bonds connected with the boron atoms (one B–N bond and two B–C bonds) are in the same plane, and the sum of the three bond angles is about 360° . As shown in Figure 1d, the B and N atoms in **BNBN-DBP** could not be crystallographically distinguished. This phenomenon was caused by the chemically asymmetric BNBN sequence (compared with the centrosymmetric BNNB sequence) in a geometrically centrosymmetric skeleton. The molecules packed

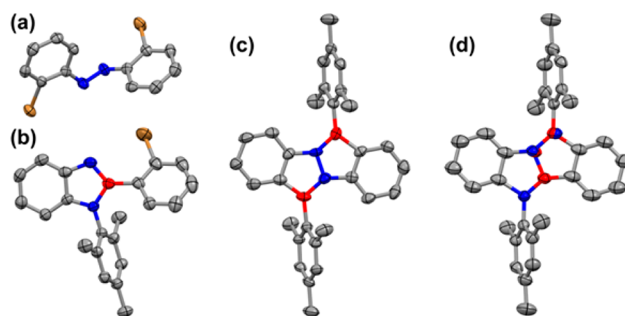


Figure 1. Single-crystal structures of (a) **2**, (b) **4**, (c) **BNNB-DBP**, and (d) **BNBN-DBP** with thermal ellipsoids shown at 50% probability. H atoms have been omitted for clarity. B and N atoms in (d) **BNBN-DBP** are not crystallographically distinguishable because of disorder. Colors: gray, carbon; red, boron; blue, nitrogen; orange, bromine.

in the crystal without any preferred orientation of the embedded BNBN sequence, thus leading to a disordered packing structure. In contrast, **BNNB-DBP** does not have this problem and provides more detailed structural information. The B–N bond lengths in **BNNB-DBP** are in the range of $1.40\text{--}1.44\text{ \AA}$, indicative of localized BN double-bond character.^{3c} The N–N bond length is around 1.42 \AA , a typical value for N–N single bonds (1.40 \AA in compound **2**). These structural features indicate that the bond length alternation in **BNNB-DBP** is similar to that in **DBP**.

To understand how the BN substitution and the orientation patterns of BN units influence the antiaromaticity of **DPB**, we performed nucleus-independent chemical shift (NICS) calculations¹⁹ at the B3LYP/6-311+G(2d,p) level. As illustrated in Figure 2, the parent **DBP** has a highly antiaromatic pentalene

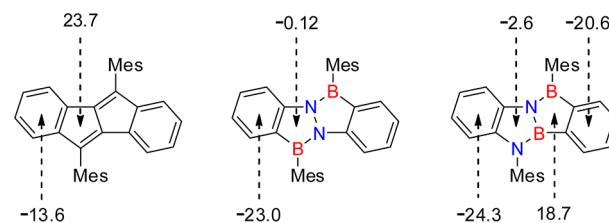


Figure 2. NICS(1_{zz}) values (in ppm) of **DBP**, **BNNB-DBP**, and **BNBN-DBP** calculated at the GIAO-B3LYP/6-311+G(2d,p) level.

core with a large positive NICS(1_{zz}) value of 23.7 ppm and moderately aromatic fused benzene rings. In **BNNB-DBP**, however, the fused benzene rings exhibit high aromaticity, whereas the BNNB-substituted pentalene core is almost nonaromatic. In contrast, the asymmetric **BNBN-DBP** has different NICS(1_{zz}) values for each ring. The fused benzene rings are aromatic, with the one on the N side much stronger. Notably, the BNBC₂ ring shows a highly antiaromatic feature (18.7 ppm), whereas the NBNC₂ ring displays weak aromaticity (-2.6 ppm).

These differences may partly relate to the lone pairs of the N atoms and the vacant p orbitals of the B atoms. The BNNC₂ ring is in principle aromatic with a total of six π electrons (Figure S4). However, when it is incorporated into the fused system of **BNNB-DBP**, the lone pair of the N atom is attracted by the extra B atom, which reduces the effective diatropic ring current and leads to lowered aromaticity. Similarly, the (anti)aromatic properties of **BNBN-DBP** can also be

rationalized by the presence of six π electrons in the NBNC₂ ring and four π electrons in the BNBC₂ ring. The aromaticity and antiaromaticity are both reduced because of the extra B or N atoms connected to each ring in **BNNB-DBP**. In addition to the effect of the heteroatoms, the global paratropic ring current from these $4n\pi$ -electron systems further reduces the aromaticity but enhances the antiaromaticity of individual rings.²⁰ These results indicate that although **DBP** and its BN-embedded derivatives possess the same $4n\pi$ electrons in total, the (anti)aromaticity of each ring is significantly modified by the BN substitution, and different BN orientation patterns lead to completely different electronic structures.

The photophysical and electrochemical properties of **BNNB-DBP** and **BNBN-DBP** were investigated by UV–vis absorption and photoluminescence spectroscopies as well as cyclic voltammetry (CV). As displayed in Figure 3, **BNNB-DBP**

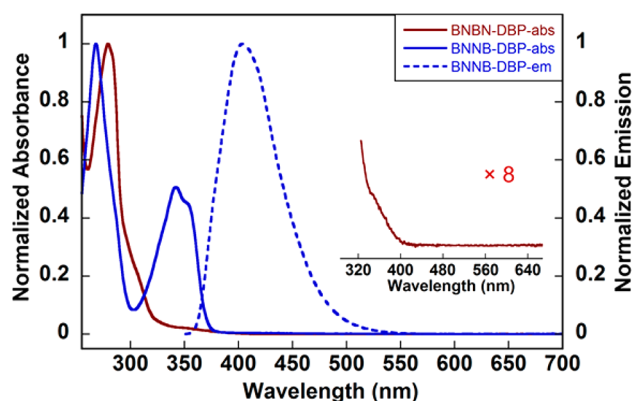


Figure 3. Absorption spectra of **BNNB-DBP** and **BNBN-DBP** and the emission spectrum of **BNNB-DBP** (excitation wavelength 342 nm) in CH₂Cl₂. The inset shows an enlarged region of the absorption spectrum of **BNBN-DBP**.

displays two main absorption bands peaking at 268 and 342 nm and an absorption onset of 375 nm, which corresponds to an optical band gap of 3.31 eV. On the other hand, **BNBN-DBP** shows a red-shifted absorption maximum at 279 nm and a very weak absorption between 320 and 400 nm (Figure 3 inset). The optical band gap deduced from the low-energy absorption onset is 3.10 eV (Figure S3), which is smaller than that of **BNNB-DBP**. Overall, both compounds revealed blue-shifted absorption onsets, that is, larger optical band gaps, relative to **DBP**.^{17d} The photoluminescence spectroscopic analysis indicated that the antiaromatic **BNBN-DBP** is nonemissive, which is similar to the case of **DBPs**.¹⁷ In contrast, **BNNB-DBP** featuring a nonaromatic pentalene core exhibited deep-blue fluorescence with an emission maximum at 403 nm and a quantum yield of 18%, which is quite unusual in pentalene derivatives. The energy levels of these two compounds were estimated by CV experiments (Figure S2). **BNNB-DBP** possesses a lower HOMO level of -5.93 eV compared with that of **BNBN-DBP** (-5.62 eV), whereas their LUMO levels are quite similar (-2.67 eV for **BNNB-DBP** and -2.60 eV for **BNBN-DBP**). The electrochemical band gaps of **BNNB-DBP** and **BNBN-DBP** are 3.26 and 3.02 eV, respectively, in good agreement with the optical band gaps.

To gain more insights into the electronic properties of **BNNB-DBP** and **BNBN-DBP** compared with their carbon analogue **DBP**, we performed density functional theory (DFT) calculations at the B3LYP/6-311G(d,p) level. As depicted in

Figure 4, BN substitution results in completely different electronic structures. First, **BNNB-DBP** and **BNBN-DBP**

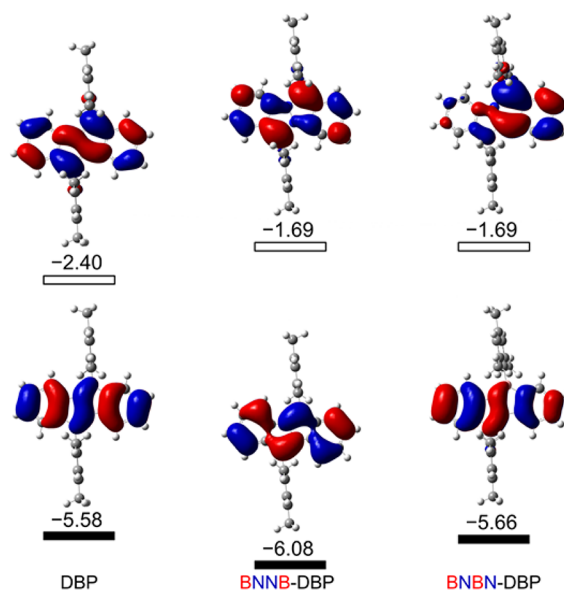


Figure 4. Frontier molecular orbitals and their energies (in eV) for **DBP**, **BNNB-DBP**, and **BNBN-DBP** calculated at the B3LYP/6-311G(d,p) level.

both exhibit larger band gaps than the parent **DBP**. **BNBN-DBP** has the same LUMO level as **BNNB-DBP** but a much higher HOMO level and thus a lower band gap, which is consistent with the experimental results as discussed above. Second, as indicated previously,^{17f} the HOMO \rightarrow LUMO transition of **DBP** is symmetry-forbidden. **BNBN-DBP** maintains a similar character, although the orbital distributions are polarized, with a larger HOMO coefficient on the N side and a severely localized LUMO on the B side (Figure 4). According to time-dependent DFT (TD-DFT) calculations, the lowest-energy absorption of **BNBN-DBP** can be assigned to the symmetry-forbidden HOMO \rightarrow LUMO transition, which exhibits an extremely low oscillator strength (f) of 0.0001 (Figure S6). In contrast, TD-DFT calculations on **BNNB-DBP** indicated that its HOMO possesses a different symmetry than that of **DBP**, while their LUMO symmetries are identical (Figure 4). Therefore, the HOMO \rightarrow LUMO transition of **BNNB-DBP** is allowed ($f = 0.2823$), corresponding to the absorption band at 342 nm (Figure 3). These results indicate that different BN substitution patterns lead to significantly distinct electronic structures, which determine their varying photophysical properties.

In summary, two BN-embedded dibenzo[*a,e*]pentalenes, **BNNB-DBP** and **BNBN-DBP**, were synthesized through multiple lithiations (on carbon and nitrogen at the same time) followed by nucleophilic substitutions. This strategy can be a promising method for the synthesis of BN-embedded conjugated molecules. Moreover, we have for the first time revealed that different BN orientation patterns significantly influence the antiaromaticity and the optical and electronic properties. These results indicate that precise control of the BN orientation pattern is of great importance for effective modulation of the chemical and physical properties of conjugated molecules with more than one BN unit embedded. Further exploration of the BN substitution strategy in

antiaromatic systems can open up new possibilities to extend the scope of antiaromatic molecules and deepen the fundamental understanding of antiaromaticity.

■ ASSOCIATED CONTENT

Supporting Information

Experimental details, synthesis, characterizations, single-crystal data (CIF), computational studies, and NMR spectra. The Supporting Information is available free of charge on the ACS Publications website at DOI: 10.1021/jacs.5b05056.

■ AUTHOR INFORMATION

Corresponding Authors

*xinliang.feng@tu-dresden.de

*muellen@mpip-mainz.mpg.de

Notes

The authors declare no competing financial interest.

■ ACKNOWLEDGMENTS

The authors sincerely thank Wen Zhang for high-resolution MALDI-TOF MS measurements and Dr. Dieter Schollmeyer (Institute for Organic Chemistry, Johannes Gutenberg University Mainz) for single-crystal X-ray structural analysis. We are grateful for the financial support from the European Research Council grant on NANOGRAPH, DFG Priority Program SPP 1459, Graphene Flagship (CNECT-ICT-604391), and European Union Projects UPGRADE and MoQuaS.

■ REFERENCES

- (1) Minkin, V. I.; Glukhovtsev, M. N.; Simkin, B. Y. *Aromaticity and Antiaromaticity: Electronic and Structural Aspects*; John Wiley & Sons: New York, 1994.
- (2) For reviews, see: (a) Wang, X.-Y.; Wang, J.-Y.; Pei, J. *Chem.—Eur. J.* **2015**, *21*, 3528. (b) Campbell, P. G.; Marwitz, A. J. V.; Liu, S. Y. *Angew. Chem., Int. Ed.* **2012**, *51*, 6074. (c) Bosdet, M. J. D.; Piers, W. E. *Can. J. Chem.* **2009**, *87*, 8. (d) Liu, Z. Q.; Marder, T. B. *Angew. Chem., Int. Ed.* **2008**, *47*, 242.
- (3) (a) Xu, S.; Mikulas, T. C.; Zakharov, L. N.; Dixon, D. A.; Liu, S.-Y. *Angew. Chem., Int. Ed.* **2013**, *52*, 7527. (b) Campbell, P. G.; Abbey, E. R.; Neiner, D.; Grant, D. J.; Dixon, D. A.; Liu, S.-Y. *J. Am. Chem. Soc.* **2010**, *132*, 18048. (c) Abbey, E. R.; Zakharov, L. N.; Liu, S.-Y. *J. Am. Chem. Soc.* **2008**, *130*, 7250.
- (4) Campbell, P. G.; Zakharov, L. N.; Grant, D. J.; Dixon, D. A.; Liu, S.-Y. *J. Am. Chem. Soc.* **2010**, *132*, 3289.
- (5) Knack, D. H.; Marshall, J. L.; Harlow, G. P.; Dudzik, A.; Szalencic, M.; Liu, S.-Y.; Heider, J. *Angew. Chem., Int. Ed.* **2013**, *52*, 2599.
- (6) (a) Wang, X.-Y.; Lin, H.-R.; Lei, T.; Yang, D.-C.; Zhuang, F.-D.; Wang, J.-Y.; Yuan, S.-C.; Pei, J. *Angew. Chem., Int. Ed.* **2013**, *52*, 3117. (b) Wang, X.-Y.; Zhuang, F.-D.; Zhou, X.; Yang, D.-C.; Wang, J.-Y.; Pei, J. *J. Mater. Chem. C* **2014**, *2*, 8152. (c) Wang, X.-Y.; Zhuang, F.-D.; Wang, R.-B.; Wang, X.-C.; Cao, X.-Y.; Wang, J.-Y.; Pei, J. *J. Am. Chem. Soc.* **2014**, *136*, 3764. (d) Wang, X.; Zhang, F.; Liu, J.; Tang, R. Z.; Fu, Y. B.; Wu, D. Q.; Xu, Q.; Zhuang, X. D.; He, G. F.; Feng, X. L. *Org. Lett.* **2013**, *15*, 5714. (e) Hashimoto, S.; Ikuta, T.; Shiren, K.; Nakatsuka, S.; Ni, J.; Nakamura, M.; Hatakeyama, T. *Chem. Mater.* **2014**, *26*, 6265. (f) Li, G.; Zhao, Y.; Li, J.; Cao, J.; Zhu, J.; Sun, X. W.; Zhang, Q. *J. Org. Chem.* **2015**, *80*, 196.
- (7) (a) Baggett, A. W.; Vasiliu, M.; Li, B.; Dixon, D. A.; Liu, S.-Y. *J. Am. Chem. Soc.* **2015**, *137*, 5536. (b) Abbey, E. R.; Lamm, A. N.; Baggett, A. W.; Zakharov, L. N.; Liu, S.-Y. *J. Am. Chem. Soc.* **2013**, *135*, 12908. (c) Braunschweig, H.; Geetharani, K.; Jimenez-Halla, J. O. C.; Schäfer, M. *Angew. Chem., Int. Ed.* **2014**, *53*, 3500. (d) Ashe, A. J., III; Fang, X. D. *Org. Lett.* **2000**, *2*, 2089.

- (8) (a) Liu, X.; Wu, P.; Li, J.; Cui, C. *J. Org. Chem.* **2015**, *80*, 3737. (b) Wisniewski, S. R.; Guenther, C. L.; Argintaru, O. A.; Molander, G. A. *J. Org. Chem.* **2014**, *79*, 365. (c) Fang, X. D.; Yang, H.; Kampf, J. W.; Holl, M. M. B.; Ashe, A. J., III. *Organometallics* **2006**, *25*, 513.
- (9) (a) Chrostowska, A.; Xu, S.; Mazière, A.; Boknevit, K.; Li, B.; Abbey, E. R.; Dargelos, A.; Graciaa, A.; Liu, S.-Y. *J. Am. Chem. Soc.* **2014**, *136*, 11813. (b) Abbey, E. R.; Zakharov, L. N.; Liu, S.-Y. *J. Am. Chem. Soc.* **2011**, *133*, 11508.
- (10) (a) Bosdet, M. J. D.; Jaska, C. A.; Piers, W. E.; Sorensen, T. S.; Parvez, M. *Org. Lett.* **2007**, *9*, 1395. (b) Lu, J. S.; Ko, S. B.; Walters, N. R.; Kang, Y.; Sauriol, F.; Wang, S. N. *Angew. Chem., Int. Ed.* **2013**, *52*, 4544.
- (11) Ishibashi, J. S. A.; Marshall, J. L.; Mazière, A.; Lovinger, G. J.; Li, B.; Zakharov, L. N.; Dargelos, A.; Graciaa, A.; Chrostowska, A.; Liu, S.-Y. *J. Am. Chem. Soc.* **2014**, *136*, 15414.
- (12) Jaska, C. A.; Emslie, D. J. H.; Bosdet, M. J. D.; Piers, W. E.; Sorensen, T. S.; Parvez, M. *J. Am. Chem. Soc.* **2006**, *128*, 10885.
- (13) Bosdet, M. J. D.; Piers, W. E.; Sorensen, T. S.; Parvez, M. *Angew. Chem., Int. Ed.* **2007**, *46*, 4940.
- (14) (a) Wang, X.-Y.; Zhuang, F.-D.; Wang, X.-C.; Cao, X.-Y.; Wang, J.-Y.; Pei, J. *Chem. Commun.* **2015**, *51*, 4368. (b) Li, G.; Xiong, W.-W.; Gu, P.-Y.; Cao, J.; Zhu, J.; Ganguly, R.; Li, Y.; Grimdale, A. C.; Zhang, Q. *Org. Lett.* **2015**, *17*, 560.
- (15) (a) Neue, B.; Araneda, J. F.; Piers, W. E.; Parvez, M. *Angew. Chem., Int. Ed.* **2013**, *52*, 9966. (b) Müller, M.; Behnle, S.; Maichle-Mossmer, C.; Bettinger, H. F. *Chem. Commun.* **2014**, *50*, 7821. (c) Hatakeyama, T.; Hashimoto, S.; Seki, S.; Nakamura, M. *J. Am. Chem. Soc.* **2011**, *133*, 18614. (d) Lepeltier, M.; Lukoyanova, O.; Jacobson, A.; Jeeva, S.; Perepichka, D. F. *Chem. Commun.* **2010**, *46*, 7007. (e) Wang, X.-Y.; Yang, D.-C.; Zhuang, F.-D.; Liu, J.-J.; Wang, J.-Y.; Pei, J. *Chem.—Eur. J.* **2015**, *21*, 8867.
- (16) For reviews, see: (a) Hopf, H. *Angew. Chem., Int. Ed.* **2013**, *52*, 12224. (b) Saito, M. *Symmetry* **2010**, *2*, 950.
- (17) (a) Li, H.; Wang, X.-Y.; Wei, B.; Xu, L.; Zhang, W.-X.; Pei, J.; Xi, Z. *Nat. Commun.* **2014**, *5*, No. 4508. (b) Zhao, J.; Oniwa, K.; Asao, N.; Yamamoto, Y.; Jin, T. *J. Am. Chem. Soc.* **2013**, *135*, 10222. (c) Chen, C.; Harhausen, M.; Liedtke, R.; Bussmann, K.; Fukazawa, A.; Yamaguchi, S.; Petersen, J. L.; Daniliuc, C. G.; Fröhlich, R.; Kehr, G.; Erker, G. *Angew. Chem., Int. Ed.* **2013**, *52*, 5992. (d) Maekawa, T.; Segawa, Y.; Itami, K. *Chem. Sci.* **2013**, *4*, 2369. (e) Levi, Z. U.; Tilley, T. D. *J. Am. Chem. Soc.* **2009**, *131*, 2796. (f) Kawase, T.; Fujiwara, T.; Kitamura, C.; Konishi, A.; Hirao, Y.; Matsumoto, K.; Kurata, H.; Kubo, T.; Shinamura, S.; Mori, H.; Miyazaki, E.; Takimiya, K. *Angew. Chem., Int. Ed.* **2010**, *49*, 7728.
- (18) During the preparation of this article, Cui and co-workers reported an elegant synthesis of BNNB-substituted benzopentalenes by electrophilic borylation from hydrazones. See: Ma, C.; Zhang, J.; Li, J.; Cui, C. *Chem. Commun.* **2015**, *51*, 5732.
- (19) Chen, Z.; Wannere, C. S.; Corminboeuf, C.; Puchta, R.; Schleyer, P. v. R. *Chem. Rev.* **2005**, *105*, 3842.
- (20) Cao, J.; London, G.; Dumele, O.; von Wantoch Rekowski, M.; Trapp, N.; Ruhlmann, L.; Boudon, C.; Stanger, A.; Diederich, F. *J. Am. Chem. Soc.* **2015**, DOI: 10.1021/jacs.5b03074.